

Measurements of He isotopic ratio in cosmic rays in the 100 MeV–1 GeV range with the PAMELA experiment

M. Casolino^{1,2}, C. De Santis¹, N. De Simone¹, V. Formato¹, N. Nikonov¹, P. Picozza¹, and the PAMELA collaboration*

¹INFN and Dept. of Physics, University of Rome Tor Vergata, Via Della Ricerca Scientifica 1, 00133, Rome, Italy

²RIKEN, Advanced Science Institute, Wako 351-0198, Japan

*<http://pamela.roma2.infn.it>

Received: 15 November 2010 – Revised: 16 February 2011 – Accepted: 17 February 2011 – Published: 26 October 2011

Abstract. The PAMELA satellite-borne experiment was launched on 15 June 2006 from the Baikonur cosmodrome and it has been collecting data since then. The apparatus comprises a time-of-flight system, a silicon-microstrip magnetic spectrometer, a silicon-tungsten electromagnetic calorimeter, an anticoincidence system, a shower tail counter scintillator and a neutron detector. The combination of these devices allows precision studies of the charged cosmic radiation to be conducted over a wide energy range (100 MeV–1 TeV) with high statistics, with particular focus on the antiparticle component. In this work we present $^3\text{He}/^4\text{He}$ isotopic ratio in the energy range from 100 MeV nucleon⁻¹ to ~ 1 GeV nucleon⁻¹. The measured abundances are compared with different interstellar/heliospheric propagation calculations which are tuned on previous proton and helium measurements.

1 Introduction

Hydrogen and helium isotopes in cosmic rays are generally believed to be of secondary origin, resulting mainly from the nuclear interactions of primary cosmic-ray protons and ^4He with the interstellar medium. A precise measurement of the isotopic composition of hydrogen and helium could provide important information about the propagation of cosmic rays in the interstellar space, since they offer better statistics than other secondaries. This can be crucial when analyzing positron and antiproton spectra, which is the primary goal of several current cosmic-ray experiments (Stephens, 1989; Wang et al., 2002).

The PAMELA experiment has been measuring since 2006 both hydrogen and helium isotopes over a wide range of time with reduced instrumental uncertainty and with no environmental systematics, such as - for instance - the residual atmosphere present in balloon experiments.

In this paper we present the isotopic composition of helium in the energy range from 0.1 to about 1 GeV nucleon⁻¹ (corresponding to rigidities from ~ 800 MV to ~ 2.5 GV) obtained from the flight data recorded until December 2008.

2 Pamela detector

PAMELA (Picozza et al., 2007) is constituted by a number of detectors with intrinsic redundancy (see Fig. 1) capable of identifying particles providing charge, mass, rigidity ($\rho = p/Ze$) and velocity ($\beta = v/c$) over a very wide energy range. Its main scientific objective is the study of the antimatter component in CR, see Boezio et al. (2009). The core of the instrument is a permanent magnet with six planes of silicon microstrip detectors for tracking particles. A three-scintillators system provides trigger, charge and time-of-flight information. A silicon-tungsten calorimeter is used for hadron/lepton separation with a shower tail catcher and a neutron detector at the bottom of the apparatus to help increase this separation. An anticounter system is used to reject spurious events in the off-line phase. The readout electronics, the interfaces with the CPU and all primary and secondary power supplies are housed around the detectors. All systems (power supply, readout boards etc.) have main/spare redundancy with the exception of the CPU which is more tolerant to failures. The apparatus is enclosed in a pressurized container located on one side of the Resurs-DK1 satellite. Total weight of PAMELA is 470 kg; power consumption is 355 W. A more detailed description of the device and the data handling can be found in Casolino et al. (2006a,b); Adriani et al. (2002).



Correspondence to: M. Casolino
(casolino@roma2.infn.it)

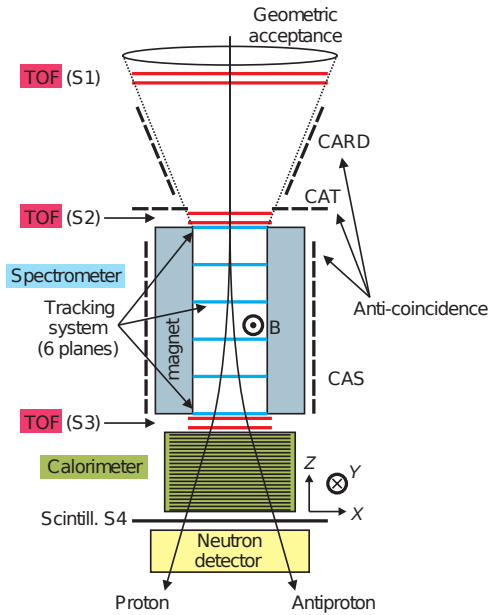


Fig. 1. A schematic overview of the PAMELA satellite experiment. The experiment stands ~ 1.3 m high and, from top to bottom, consists of a time-of-flight (ToF) system (S1, S2, S3 scintillator planes), an anticoincidence shield system, a permanent magnet spectrometer (the magnetic field runs in the y -direction), a silicon-tungsten electromagnetic calorimeter, a shower tail scintillator (S4) and a neutron detector.

3 Analysis

The high inclination (70°) orbit of the Resurs-DK1 satellite and the long mission duration allow PAMELA to study low energy particles (down to 50 MeV) investigating several aspects of the solar and terrestrial environment.

To select the primary (galactic) component we evaluated the local geomagnetic cutoff G in the Störmer approximation (Shea et al., 1987). The value of $G = 14.9/L^2$ - valid for vertically incident particles - is estimated using the IGRF magnetic field model along the orbit; from this the McIlwain L shell is calculated (igr, 2005). Particles were selected requiring $\rho > 1.3 G$ to remove any effect due to directionality in the detector and Earth's penumbral regions.

For the measurement of ratios as functions of kinetic energy the geomagnetic cutoff cut is applied considering the same geographical region for the two isotopes requiring $\rho^*(E) > 1.3 G$, where $\rho^*(E)$ is the lowest rigidity between the two isotopes having kinetic energy E .

We have selected events that do not produce secondary particles by requiring a single track fitted within the spectrometer fiducial acceptance and a maximum of one paddle hit in the two top scintillators of the ToF system. The hits in the two scintillators must match the extrapolated trajectory from the tracker. Albedo particles are rejected requiring $\beta > 0$.

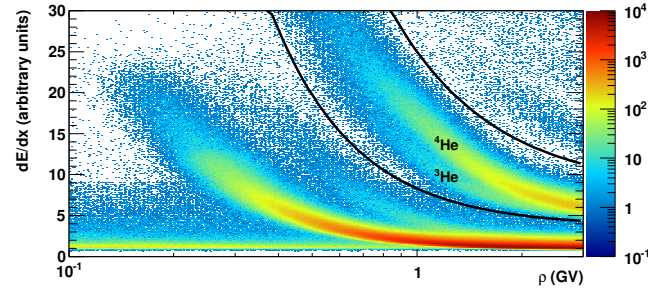


Fig. 2. Energy loss in tracker (mean in all planes hit) vs tracker rigidity for positively charged particles. The Proton and Helium bands are clearly visible. The black lines represent cuts used to select He nuclei.

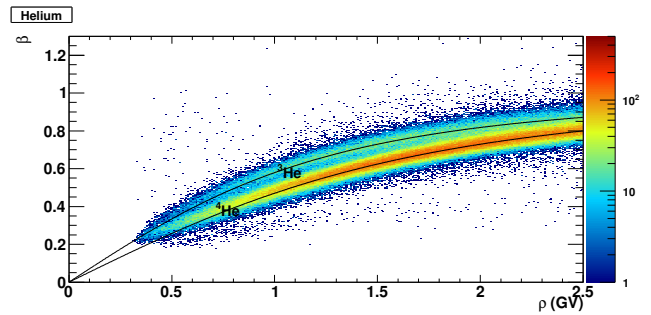


Fig. 3. Mass separation for $Z = 2$ particles with the β vs. rigidity method. The black lines represent the theoretical curves from Eq. (1)

3.1 Helium selection

The measurement of the average energy released in the tracker planes for a given event at a given rigidity can be used to discriminate between different particles since energy loss of a charged particle through matter follows the Bethe Block formula, $dE/dx \propto Z^2/\beta^2$ (neglecting logarithmic terms). In Fig. 2 is shown the energy loss in the tracker as a function of the particle rigidity. The top band is due to helium nuclei which have energy loss in the tracker $Z^2 = 4$ times the protons, identified in the central band. The band at the bottom left of Fig. 2 is due to positrons, relativistic also at low rigidities and the background of pion and secondary particles. The black lines show the energy dependent cuts used to select the helium sample.

Cuts in the energy loss (dE/dx) vs rigidity remove positrons, pions, hydrogens and particles with $Z > 2$ as shown in Fig. 2.

3.2 Isotope separation

To separate ${}^3\text{He}$ from ${}^4\text{He}$ we have taken the $1/\beta$ distribution (described by a Gauss function) at fixed rigidity. As shown in Fig. 3 the different masses of the isotopes guarantee a sep-

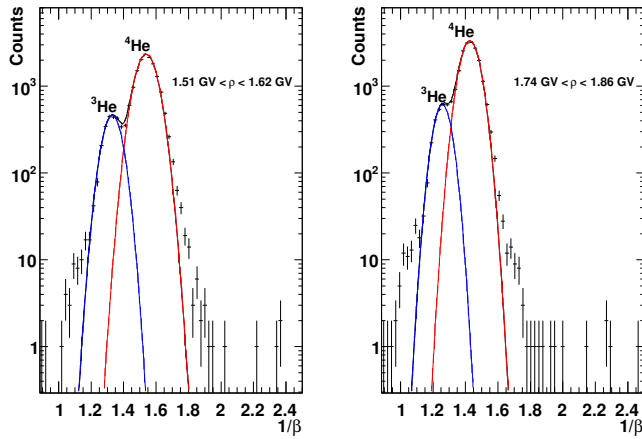


Fig. 4. Examples of isotopic separation between ^3He and ^4He at fixed rigidity range.

aration (decreasing with energy) in the $1/\beta$ distribution according to

$$\frac{1}{\beta} = \sqrt{1 + \frac{A^2 m_p^2}{Z^2 \rho^2}}. \quad (1)$$

A simulation has shown that this method can be safely applied up to rigidities of 2.5 GV, where the peak of the ^3He gaussian is still above the background from ^4He events; below this value the systematic uncertainty is less than 5%.

Inside each bin we estimate the number of particles by fitting the total $1/\beta$ distribution using the sum of two Gaussian functions (Fig. 4)

$$f(x) = A \cdot \exp\left[-\frac{(x - \mu_1)^2}{2\sigma_1^2}\right] + B \cdot \exp\left[-\frac{(x - \mu_2)^2}{2\sigma_2^2}\right] \quad (2)$$

(where $x = 1/\beta$ at fixed rigidity) with the Maximum Likelihood method assuming the mean values of the two gaussians (μ_1 and μ_2) from Eq. (1). The ratio R is then evaluated as $R = A\sigma_1/B\sigma_2$.

In order to have isotopic ratios as function of kinetic energy we fix the kinetic energy bins of the final ratio and calculate the corresponding rigidity intervals for each species. Two different rigidity binning (one for each isotope) are selected in such a way that the n -th rigidity bin will always correspond to the same kinetic energy range.

In the rigidity dependent ratios the selection efficiency (which depends on the particle rigidity) is the same for all the isotopes of a given element. This assumption is no longer valid when measuring kinetic energy isotopic ratios since, due to the different mass, at a given kinetic energy value correspond different rigidities for the isotopes; thus the selection efficiency has been corrected by a factor equal to the ratio of the efficiencies estimated by the analysis on proton and helium absolute fluxes. This correction is less than 10% below $300 \text{ MeV nucleon}^{-1}$ and less than 1% above $300 \text{ MeV nucleon}^{-1}$.

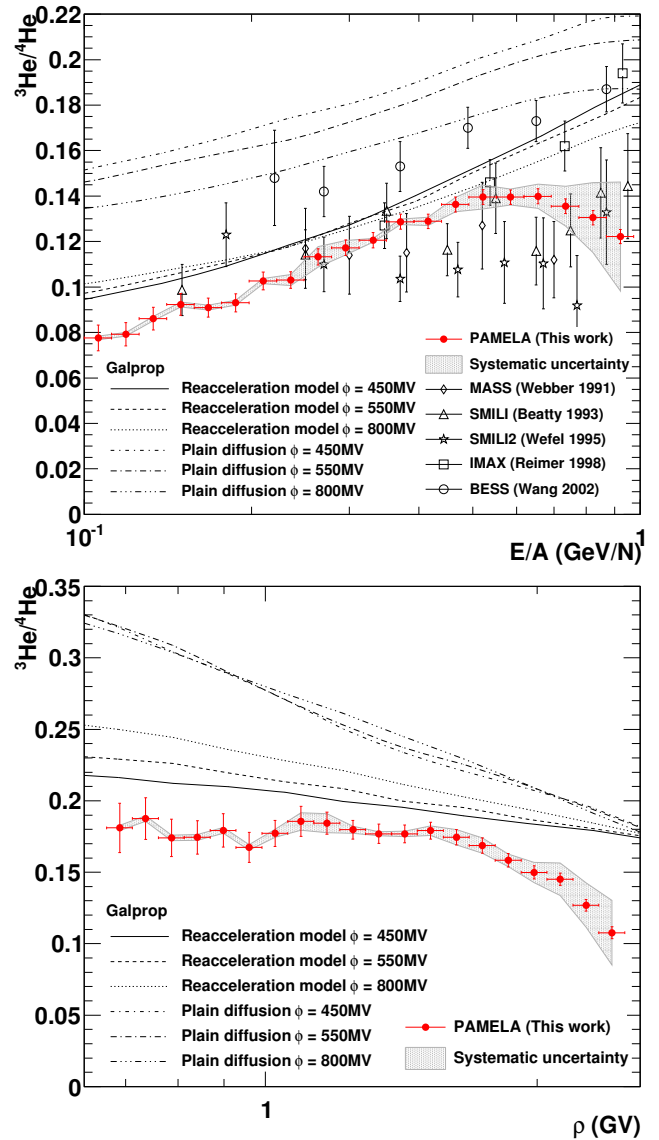


Fig. 5. $^3\text{He}/^4\text{He}$ ratio R as a function of kinetic energy per nucleon (top) and rigidity (bottom). The error bars show the statistical error, and the shaded regions show the systematic uncertainty of the measure. Previous measurements (Wang et al., 2002; de Nolfo et al., 2000; Reimer et al., 1998; Webber et al., 1991; Beatty et al., 1993) are shown together with theoretical predictions by Strong and Moskalenko (Trotta et al., 2011).

3.3 Contribution of secondary particles - top of the payload correction

Helium nuclei may be lost due to hadronic interactions in the 2 mm Al thick pressurized container and the top scintillator detectors; the correction to the ratio due to particles lost and the contribution of ^3He from ^4He inelastic scattering has been estimated to be less than 1% and has been included in the systematic uncertainty of the measurement.

Table 1. GALPROP parameters for the models considered as described in Ptuskin et al. (2006). Injection index are below/above the break rigidity and the diffusion coefficient for the plain diffusion model is below/above $\rho_0 = 3$ GV.

	Nuclei injection index	Break rigidity (GV)	Diffusion coefficient	
			value at $\rho = 3$ GV ($\text{cm}^2 \text{s}^{-1}$)	index
Reacceleration model	1.82/2.36	4	$5.2 \cdot 10^{28}$	0.34
Plain diffusion model	2.30/2.15	40	$2.2 \cdot 10^{28}$	0/0.6

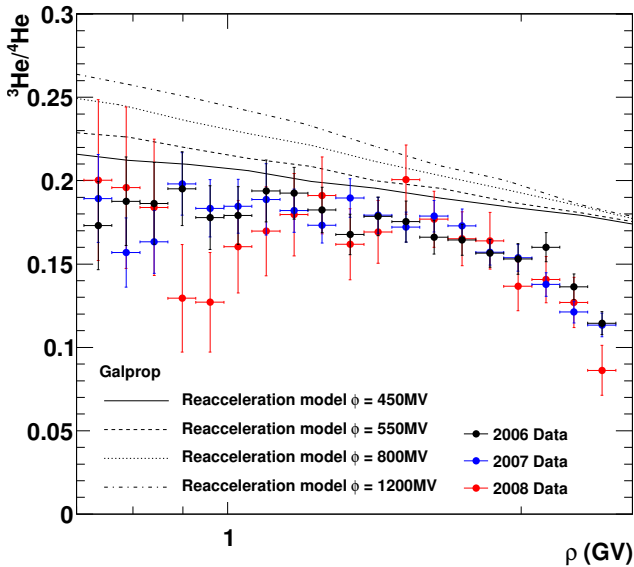


Fig. 6. Time variations of $^3\text{He}/^4\text{He}$ ratios as functions of rigidity. Data show no sign of solar modulation during the examined period.

4 Results

In Fig. 5 the $^3\text{He}/^4\text{He}$ ratio as a function of both kinetic energy per nucleon and rigidity is shown. Previous experimental measurements are in agreement with PAMELA data, though they were affected by additional sources of systematic error like the contribution of residual atmosphere present in balloon experiments. The curves show the prediction of diffusive reacceleration model and plain diffusion model evaluated with GALPROP (Trotta et al., 2011) for different values of the solar modulation parameter (450, 550, and 800 MV) in the spherical force-field approximation (Gleeson and Axford, 1968).

Figure 6 shows the time evolution of the isotopic ratio in the years between 2006 and 2008. All measurements have been taken at the minimum activity of Solar cycle 23 so, as expected from models, there is no evident change with time. Even at solar maximum condition (Fig. 6, top curve) the difference with respect to solar minimum condition is $\sim 20\%$ at low energy and decreases with increasing rigidity.

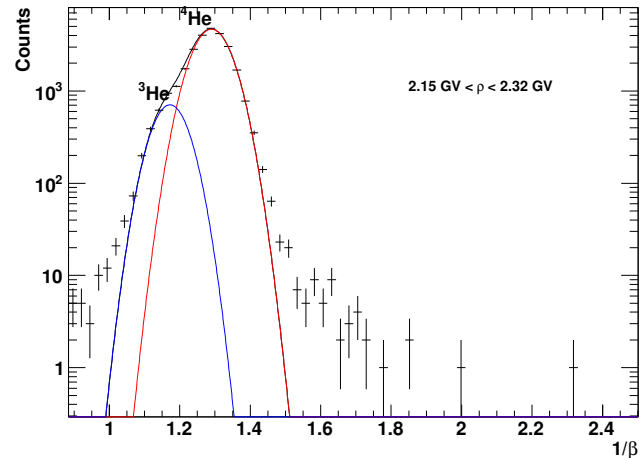


Fig. 7. Example of isotopic separation between ^3He and ^4He in the last bins of this analysis. The contribution from ^3He is still visible in the $1/\beta$ distribution.

5 Conclusions

In this work we have shown the measurement of $^3\text{He}/^4\text{He}$ taken at Earth with PAMELA. It is possible (Fig. 7) to see that the amount of ^3He decreases above $600 \text{ MeV nucleon}^{-1}$, in disagreement with theoretical models. Further data will be needed to clarify the cause of this discrepancy, for instance a future comparison of D/H ratio will help to better understand the phenomena taking place in galactic propagation.

Edited by: M. Potgieter

Reviewed by: two anonymous referees

References

- International Geomagnetic Reference Field, Tech. rep., IAGA, 2005.
- Adriani, O., Ambriola, M., Barbarino, G., et al.: The PAMELA experiment on satellite and its capability in cosmic rays measurements, Nucl. Instr. Meth. Phys. Res. A, 478, 114–118, doi:10.1016/S0168-9002(01)01726-0, 2002.
- Beatty, J. J., Ficenec, D. J., Tobias, S., et al.: The cosmic-ray He-3/He-4 ratio from 100 to 1600 MeV/amu, Astrophys. J., 413, 268–280, doi:10.1086/172994, 1993.

- Boezio, M., Pearce, M., Picozza, P., et al.: PAMELA and indirect dark matter searches, *New J. Phys.*, 11, doi:10.1088/1367-2630/11/10/105023, 2009.
- Casolino, M., Altamura, F., Basili, A., et al.: The PAMELA storage and control unit, *Adv. Space Res.*, 37, 1857–1861, doi:10.1016/j.asr.2005.06.012, 2006a.
- Casolino, M., de Pascale, M. P., Nagni, M., et al.: YODA++: A proposal for a semi-automatic space mission control, *Adv. Space Res.*, 37, 1884–1888, doi:10.1016/j.asr.2005.06.033, 2006b.
- de Nolfo, G. A., Barbier, L. M., Christian, E. R., et al.: A measurement of cosmic ray deuterium from 0.5–2.9 GeV/nucleon, in: *Acceleration and Transport of Energetic Particles Observed in the Heliosphere*, edited by: R. A. Mewaldt, J. R. Jokipii, M. A. Lee, E. Möbius, and T. H. Zurbuchen, American Inst. Phys. Conf. Series, 528, 425–428, doi:10.1063/1.1324352, 2000.
- Gleeson, L. J. and Axford, W. I.: Solar Modulation of Galactic Cosmic Rays, *Astrophys. J.*, 154, 1011, doi:10.1086/149822, 1968.
- Picozza, P., Galper, A. M., Castellini, G., et al.: PAMELA - A payload for antimatter matter exploration and light-nuclei astrophysics, *Astropart. Phys.*, 27, 296–315, doi:10.1016/j.astropartphys.2006.12.002, 2007.
- Ptuskin, V. S., Moskalenko, I. V., Jones, F. C., Strong, A. W., and Zirakashvili, V. N.: Dissipation of Magnetohydrodynamic Waves on Energetic Particles: Impact on Interstellar Turbulence and Cosmic-Ray Transport, *Astrophys. J.*, 642, 902–916, doi:10.1086/501117, 2006.
- Reimer, O. Menn, W., Hof, M., et al.: The Cosmic-Ray $3\text{He}/4\text{He}$ Ratio from 200 MeV per Nucleon to 3.7 GeV per Nucleon, *Astrophys. J.*, 496, 490, doi:10.1086/305358, 1998.
- Shea, M. A. Smart, D. F., Gentile, L. C., et al.: Estimating cosmic ray vertical cutoff rigidities as a function of the McIlwain L-parameter for different epochs of the geomagnetic field, *Phys. Earth and Planetary Interiors*, 48, 200–205, doi:10.1016/0031-9201(87)90145-2, 1987.
- Stephens, S. A.: Deuterium and He-3 in cosmic rays, *Adv. Space Res.*, 9, 145–148, doi:10.1016/0273-1177(89)90322-0, 1989.
- Trotta, R., Jóhannesson, G., Moskalenko, I. V., et al.: Constraints on Cosmic-ray Propagation Models from A Global Bayesian Analysis, *Astrophys. J.*, 729, 2, 106, 2011.
- Wang, J. Z., Seo, E. S., Anraku, K., et al.: Measurement of Cosmic-Ray Hydrogen and Helium and Their Isotopic Composition with the BESS Experiment, *Astrophys. J.*, 564, 244–259, doi:10.1086/324140, 2002.
- Webber, W. R., Golden, R. L., Stochaj, S. J., Ormes, J. F., and Strittmatter, R. E.: A measurement of the cosmic-ray H-2 and He-3 spectra and H-2/He-4 and He-3/He-4 ratios in 1989, *Astrophys. J.*, 380, 230–234, doi:10.1086/170578, 1991.